Advances in Concrete Construction, *Vol. 16, No. 5 (2023) 255-267*
https://doi.org/10.12989/acc.2023.16.5.255

A comparative study on the mechanical properties of ultra early strength steel fiber concrete

Yi-Chun Lai*[1], Ming-Hui Lee [2a] and Yuh-Shiou Tai [3b]

[1] *Department of Civil Engineering, Military Academy, Kaohsiung, 83059, Taiwan, Republic of China*
[2] *Department of Civil Engineering, National Pingtung University of Science and Technology, Pingtung, 912301, Taiwan, Republic of China*
[3] *HiPer Fiber LLC, 25920 Northline Commerce Dr., STE 404, Taylor, Michigan, 48180, USA*

(*Received June 29, 2023, Revised April 29, 2024, Accepted May 10, 2024*)

Abstract. The production of ultra-early-strength concrete (UESC) traditionally involves complexity or necessitates high-temperature curing conditions. However, this study aimed to achieve ultra-early-strength performance solely through room-temperature curing. Experimental results demonstrate that under room-temperature (28°C) curing conditions, the concrete attained compressive strengths of 20 MPa at 4 hours and 69.6 MPa at 24 hours. Additionally, it exhibited a flexural strength of 7.5 MPa after 24 hours. In contrast, conventional concrete typically reaches around 20.6 MPa (3,000 psi) after approximately 28 days, highlighting the rapid strength development of the UESC. This swift attainment of compressive strength represents a significant advancement for engineering purposes. Small amounts of steel fibers (0.5% and 1% by volume, respectively) were added to address potential concrete cracking due to early hydration heat and enhance mechanical properties. This allowed observation of the effects of different volume contents on ultra-early-strength fiber-reinforced concrete (UESFRC). Furthermore, the compressive strength of 0.5% and 1% UESFRC increased by 16.3% and 31.3%, respectively, while the flexural strength increased by 37.1% and 47.9%. Moreover, toughness increased by 58.2 and 69.7 times, respectively. These findings offer an effective solution for future emergency applications in public works.

Keywords: flexural strength growth rate; steel fibers; toughness growth value; ultra-early-strength fibers reinforced concrete

1. Introduction

High-early-strength fiber concrete (HESFC) has been widely used in civil engineering construction projects, such as precast bridge components and airport runways (Ghosh *et al*. 2021, Wu *et al*. 2016, Nayaka *et al*. 2018, Johnston 1992). This type of concrete has excellent workability and promptly developed compressive strength. The addition of fibers can increase the tensile strength of concrete and provide an adequate solution for constructing and maintaining infrastructures. Urgent construction projects often use this type of concrete to achieve the desired strength quickly, accelerating the construction process and minimizing its impact on public transportation (Johnston 1992). Researchers have utilized various mixtures and curing conditions to enable concrete to attain early strength within a designated period, including low water-to-cement (W/C) ratios and chemical or mineral admixtures to reduce water content and induce hydration (Wu *et al*. 2016, Nayaka *et al*. 2018, Golaszewski *et al*. 2019, Eskandarsefat 2018, Tang 2021, Engbert and Plank 2021). Concrete achieved the desired strength for early-strength concrete rapidly and efficiently by utilizing an early-strength agent (E.S.A.) (Wu *et al*. 2016, Golaszewski *et al*. 2019). Over the past few years, numerous variations of early strength agents have been developed. During the initial mixing phase, when traditional ESA polymer is combined with naphthalene sulfonic acid or melamine, it gets absorbed by the cement and forms a coating on the cement particles. This coating enhances the surface charge of the cement particles, leading to repulsive forces between them. As a result, the cement particles disperse more effectively, enhancing the efficiency of the cement hydration reaction and improving the water reduction effect. (Nkinamubanzi *et al*. 2016, Wu *et al*. 2021) Recently developed early-strength agents employ the concept of a zero-energy system, primarily by combining new polymers to ensure good workability. Unlike traditional early-strength agents that rely on intermolecular repulsion for dispersion in water, ESA(I) used in this study mainly combines carboxylate ether molecules. These molecules comprise highly flexible long chains with opposite functional groups and long hydrophilic side chains. These side chains form a three-dimensional barrier between cement particles and accelerate hydration reactions (Flatt and Schober 2012, Xia *et al*. 2020). In the meantime, the utilization of nanoparticles as crystal seeds in an early-strengthening agent, where calcium silicate hydrate (C-S-H) is the primary component, can greatly enhance the hardening of concrete and accelerate the initial strength development. This approach offers a more efficient means of promoting the hydration reaction of cement. The effective utilization of polycarboxylate and nanoparticle

*Corresponding author, Lecturer,
E-mail: rocma84111@smail.nchu.edu.tw
[a] Ph.D., Professor, E-mail: MHLee61@mail.npust.edu.tw
[b] Ph.D., E-mail: yuhshiou.tai@gmail.com

ISSN: 2287-5301 (Print), 2287-531X (Online)

early strength agents has demonstrated the ability to attain compressive strengths of 13 MPa just 6 hours after placement and approximately 18 MPa after 24 hours, all without steaming (Kanchanason and Plank 2018). Moreover, it enables the resumption of traffic within a mere 4 hours of casting, as observed in the study conducted by Bury (Bury and Nmai 2005). Furthermore, innovative approaches have been employed to enhance concrete's durability. One such method involves raising the temperature of the mixing water or improving the surface adhesion between coarse aggregates and mortar (Golaszewski *et al*. 2019, Eskandarsefat 2018). Among these techniques, elevating the curing temperature is commonly used for expediting the concrete's hydration process. This expedites the formation of calcium silicate hydrate (C-S-H), a vital component responsible for early strength development (Nayaka *et al*. 2018, Golaszewski *et al*. 2019, Kumar *et al*. 2021).

While early strength concrete (ESC) is commonly used in precast and transportation construction projects, it may not be sufficient for specific specialized projects. For instance, military airport runway paving requires concrete to have specific compressive and flexural strengths within a limited time, while also exhibiting excellent anti-cracking properties and the ability to resist reflective cracks resulting from the interaction between ambient temperature changes and vehicle loads. However, the rapid increase in hydration heat during the curing process may cause concrete cracking, which could reduce compressive strength and durability (Golaszewski *et al*. 2019, Li and Li 2011, Wang and Li 2006, Kim *et al*. 2018). UESFRC has been developed to address this issue by adding steel fibers to the existing ultra-early strength concrete. The addition of steel fibers enhances the flexural strength of the concrete and prevents damage such as cracking or corner fracture, while still achieving a compressive strength of over 21 MPa within 4 hours and reaching more than 50% of the design strength within 24 hours (Liu *et al*. 2020, Yasin *et al*. 2017). Moreover, incorporating steel fibers into UESFRC increases its flexural strength and ductility and inhibits shrinkage (Bhat and Khan 2018, Ghosh *et al*. 2021). It is helpful in designing seismic applications. The crack formation, size, and expansion in steel fiber-reinforced concrete beams are much more resistant to bending moments. It is believed that beams with steel fibers should be favored and even become standard practice (Altun *et al*. 2007). Barros *et al*. (2013) examined the benefits of incorporating steel fibers in enhancing the shear performance of shallow beams that experienced shear failure. The empirical findings demonstrate that including steel fiber reinforcement substantially enhanced the shear capacity of high-strength concrete layers. A study by Kaïkea *et al*. (2014) found that the energy absorbed by the beam specimen during the test at 2% fiber integration was 33 times higher than the flexural toughness of plain concrete. Furthermore, in the study conducted by Haido *et al*. (2021), it was observed that incorporating extended steel fibers led to an enhancement in the fracture energy of the fiber-reinforced concrete beams during impact testing. Concurrently, other research has demonstrated that steel fibers could effectively improve the performance of concrete, reducing the members' size, decreasing the amount of construction materials used and being more eco-friendly (Kumar *et al*. 2014, Pansuk *et al*. 2017). However, the excessive addition of steel fibers may limit its fluidity due to fiber balling (Kontoni *et al*. 2023). Therefore, the Unified Facilities Criteria 3-260-01 (UFC 2019) specifies the maximum quantity of steel fibers that can be added without compromising the workability of concrete. In recent studies, researchers have employed various techniques to enhance the performance of UESFRC. Ananyachandran and Vasugi (2022) proposed an effective approach for achieving sustainable high-early strength concrete by incorporating pozzolans and a combination of accelerators into conventional concrete. Their experimental results indicated that ordinary Portland cement concrete, substituted with 15% Metakaolin and accelerators, exhibited improved early strength and durability performance. Similarly, Sunarno *et al*. (2023) utilized abundant fly ash to produce high-early-strength concrete. Their research demonstrated that incorporating 50% fly ash in the cementitious material, along with an effective water reducer and accelerator, enhanced initial compressive strength. All samples of high-early-strength concrete met established standards, indicating that appropriate chemical admixtures effectively mitigated fly ash limitations in this application.

Accelerating concrete strength gain is essential for various construction projects, and steam curing has been the traditional method of achieving this. However, implementing heat curing for large castings can be challenging and costly. As such, there is a need to develop a concrete mixture that can reach the required strength at ambient temperatures. This would enable the use of UESFRC in a wider range of engineering projects without the need for costly and complex curing procedures.

This study developed a type of UESFRC to achieve a compressive strength of 20.6 MPa (3000 psi) within 4 hours under atmospheric temperature conditions. The influence of different ages and steel fiber contents on the properties of UESFRC was examined. The mechanical properties of UESFRC were analyzed by assessing the compressive strength growth rate and residual flexural strength reduction rate. The experiments' results showed that adding steel fibers to the concrete significantly improved its flexural properties and toughness, which are essential characteristics of UESFRC.

2. Experimental program

2.1 Specimen preparation

The properties of UESFRC are affected by various variables such as the water-to-cement ratio, proportions of admixtures, aggregate type and gradation, and the chemical composition of cement. Portland type I cement was utilized as the primary binding material because it is more widely available and cost-effective compared to Portland type III cement. The materials used in the mixture comprised silica fume, natural sand, natural coarse aggregate with two

Table 1 Compositions of the UESFRC mixtures

Type	Mix ingredients(kg/m^3)									
	Cement	Silica fume	Fine aggregate	Coarse aggregate		Steel fiber*	Admixture**			w/c
				2 cm_60%	1 cm_40%		HRWR	ESA(I)	ESA(II)	
UESC	600	60	648.9	537.6	358.4	0	1%	2%	7%	27.5%
UESFRC 0.5%			643.3	533	355.4	0.5%				
UESFRC 1%			605.9	502	334.7	1%				

**Volume fraction of steel fibers
**The amount of admixtures added is the solid content

particle sizes, water, superplasticizers, early-strength agents, and straight micro steel fibers. The composition of the UESFRC mixtures is provided in Table 1. To attain the desired strength within 4 hours, a low water-cement ratio of 0.275 was used. To evaluate the impact of added steel fiber on concrete flexural strength, three steel fiber volume fractions were tested: 0%, 0.5%, and 1%, identified as UESC, UESFRC 0.5%, and UESFRC 1%, respectively. The decision to explore two different fiber percentages, specifically 0.5% and 1%, was made with the goal of optimizing the performance of the fiber-reinforced concrete while addressing potential issues such as balling due to excessive fiber content. Considering these factors, we opted to cap the steel fiber content at a maximum of 1% in our study to mitigate the risk of balling while still leveraging the advantages of fiber reinforcement. By examining both 0.5% and 1% ratios, the authors aimed to balance steel fiber content and concrete performance. The 0.5% ratio represents a cautious approach, ensuring minimal fiber usage while still providing reinforcement. Conversely, the 1% ratio allows us to investigate the impact of slightly higher fiber content, offering insights into whether incremental increases in fiber volume yield significant enhancements in concrete properties.

This research investigated the effectiveness of using micro silica fume with a high SiO_2 content and bulk density of 500-700 kg/m^3. The pozzolanic reaction of silica fume with the calcium hydroxide produced by cement hydration generated cementitious constituents that filled the interfacial transition zone, leading to improved paste viscosity and uniform gradation. The gradation was achieved using natural sand and two grades of coarse-surfaced gravel with average particle diameters of 1.0 and 2.0 cm, respectively, in a 60:40 ratio to achieve a uniform gradation design. A high-range water reducer (HRWR) of a polycarboxylate base with long side chains was added to improve paste fluidity. During the initial mixing stage, the repulsive force dispersed the cement particles, and the side chains formed solid barriers between the cement particles, stabilizing the dispersing effect and separating the cement particles.

In this study, the UESFRC utilized two special agents to achieve super early-strength properties, eliminating the need for heat treatment. These agents, known as early-strength agents (ESA), were employed to enhance both early and late-stage strength. The traditional ESA, such as nesulfonic acid or Melamine, accelerates the hydration reaction of cement in concrete. When mixed initially, the polymer of the ESA is absorbed by the cement and

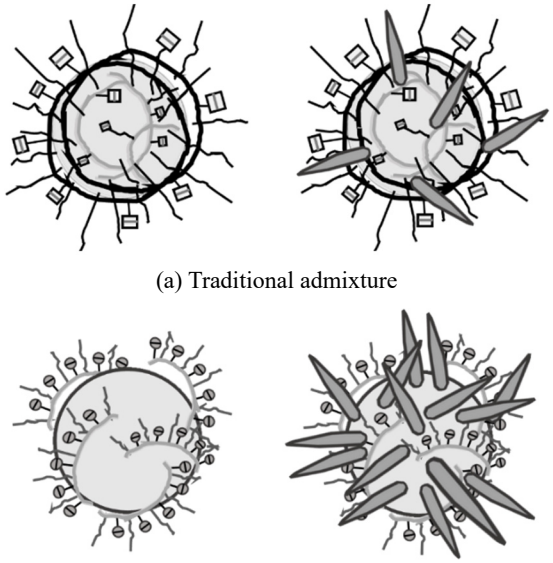

(a) Traditional admixture

(b) Molecules of the new polymer

Fig. 1 The hydration of cement with: (a) traditional admixture; and (b) molecules of the new polymer (Lee 2020)

encapsulates the cement particles. This process increases the surface charge of the cement particles, leading to mutual repulsion and improved dispersion. As a result, the efficiency of the cement hydration reaction is enhanced, and water reduction is improved (Nkinamubanzi *et al*. 2016), as depicted in Fig. 1(a).

The concept of ESA (I) is based on the zero energy system, combining glenium curing without steam and rheodynamic concrete placement without vibration (Anderson 2001). This ESA exhibits similar characteristics to traditional ESA in terms of its polymer molecules rapidly diffusing in water to generate mutual repulsion and provide dispersion. Additionally, its composition includes polycarboxylic acid ether molecules with flexible long chains containing negative functional groups and long hydrophilic side chains. These components create a three-dimensional barrier effect between cement particles, facilitating unobstructed hydration reaction and achieving rapid hydration (Flatt and Schober 2012, Xia *et al*. 2020, Kanchanason and Plank 2018), as illustrated in Fig. 1(b).

Adding ESA II to concrete can enhance durability and accelerate early strength development. ESA II contains nano-sized calcium silicate hydrate (C-S-H) particles,

Fig. 2 Steel fibers

Fig. 3 Simulating the surface environment in the construction site by polystyrene boxes

which act as nucleation sites to enhance cement hydration. Using carefully designed polymer molecules, it regulates cement hydration reactions, effectively utilizing the heat of hydration generated during the process to achieve high strength without additional external heat energy. These agents reduced the early curing time of the concrete and promoted cement hydration by mainly consisting of C-S-H hydrate nanoparticles as seed crystals, which improved concrete hardening and strength development.

Short fibers offer distinct advantages over their longer counterparts. Their reduced susceptibility to balling minimizes the risk of compromising concrete uniformity and mechanical properties. Furthermore, short fibers promote effective dispersion throughout the concrete mix, enhancing crack resistance and overall performance. This choice was made thoughtfully, considering the need to optimize fiber reinforcement while ensuring optimal concrete properties. These fiber specifications met the standards of ASTM 820 type I fibers, with tensile strength greater than 2850 MPa. Fig. 2 depicts the steel fibers used in this study.

In order to maintain consistent water content and prevent variations caused by differences in aggregate water content, fully dry fine aggregate and saturated-surface-dry coarse aggregate should be used for trial mixing. However, the timing, sequence, and mixing time of admixture addition can significantly impact the development of early strength. If the early-strength agent is added too early, workability may decrease due to the insufficient reaction time of the superplasticizer. Conversely, if the agent is added too late, the admixture distribution may not be uniform. As such, mixing protocols must be carefully controlled when working with ultra-early strength concrete (UESC). Since no specialized curing method was used in this study, the material mixing process was closely monitored to achieve the desired strength.

The optimal mixing procedure for UESFRC was determined after multiple trials to control the quality of the material. First, cement, silica fume, sand, and saturated-surface-dry coarse aggregate were dry mixed in a mixer for 5 minutes. Then, superplasticizers and premixing water solutions were added and mixed for 2 minutes. ESA (I) was added to improve the late-stage strength and mixed for 8 minutes. Finally, ESA (II) was added to improve the early strength.

To ensure the uniform distribution of ESA (I) in the paste and provide sufficient reaction time, the pouring sequences and time intervals of the two agents were strictly controlled. Once the paste exhibited desirable workability, ESA (II) was added, taking into account the reaction time of approximately 15-20 minutes. Next, straight micro steel fibers and the ESA (II) agent were introduced, and the paste was continuously mixed for 5-8 minutes to guarantee the uniform distribution of the steel fibers. During the pouring and casting procedures, the slump and fluidity of concrete were measured through slump tests based on the ASTM C230 standards.

Once the mixing process was finished, the paste was poured into cylindrical molds with a diameter of 150 mm and length of 300 mm, as well as beam testing molds with a size of 100 mm × 100 mm × 300 mm. To maintain surface temperature and prevent any loss due to exposure to air, the specimens were put in polystyrene boxes to imitate the environment at the construction site. These conditions were maintained until the testing phase. The preservation of the specimens can be seen in Fig. 3.

2.2 Equipment and experimental procedures

In this study, compressive tests were performed on materials that were aged for varying lengths of time, including 4 hours, 6 hours, 1 day, 3 days, 7 days, 14 days, and 28 days. The compressive test was used to perform with a 200-t automatic compressive testing machine. The loading speed was kept constant at 20 MPa/min until the specimen was completely destroyed and the maximum compressive strength was obtained. The data was collected and recorded by a computer.

Similarly, flexural tests were conducted on materials aged for 1, 3, 7, 14, and 28 days, using an MTS universal hydraulic testing machine (1000-kN). The loading speed was set at 0.06 mm/min for loading at a constant velocity, following ASTM C1609 standards. During the test, the load cell of the testing machine measured the applied force, and the center point deflection was measured using a linear variable differential transformer (LVDT). Both the loading and deflection signals were transmitted synchronously to a data-acquisition system. The sampling rate was set to 2 Hz.

The initial compressive test demonstrated that the cement continued to hydrate during the first three days, resulting in a considerable increase in the strength of the concrete while keeping the specimen warm. However, the flexural test took a longer time, about 20-30 minutes. Once the specimens were taken out of the thermostat, the rapid cooling of the test specimen compromised the strength development, resulting in a reduced strength compared to

the original strength. As a result, obtaining the flexural strength accurately at a specific time point was not feasible due to the lengthy testing process. It is worth noting that the concrete strength increased during the test. Time differences between tests on different sets of samples may have resulted in variations in the data, so flexural experiments at 4 and 6 hours of age were not considered in this study. Previous studies have reported similar challenges in obtaining the flexural strength of concrete due to the lengthy testing process and the complexity of the test method (Dai *et al*. 2019). However, compressive strength is a more reliable and straightforward test for early strength evaluation, and it is commonly used in many concrete-related applications (Wang *et al*. 2018).

2.3 Analytical method of flexural testing

The ASTM C78/C78M testing standard was utilized to conduct flexural tests, using standard specimens with dimensions of 100 × 100 × 350 mm and a gauge length of 300 mm. To perform the test, a beam specimen was positioned on two bearings with a span length, equivalent to three times the depth of the beam specimen. Vertical loads were then applied on the two bearings at identical intervals above the specimen within the span, as shown in Fig. 4. An LVDT was placed at the middle of the specimen to measure the center point deflection of the loaded beam specimen, and a constant uniform bending moment was applied under a constant force between the two loading blocks to enable measurement of the maximum bending stress for torque failure (ASTM C78/C78M 2021). Compared to single-point flexural testing, which yields different shear and torque values at each point on the span, three-point flexural testing is more stable and useful for analyzing flexural strength. In this study, the relationship between flexural loading and flexural strength was determined by utilizing the bending moment diagram of the loading area, as presented by the following equation

$$f = \frac{PL}{bd^2} \tag{1}$$

where f is the flexural strength, P is the applied load, L is the span length, b is the beam width, and d is the beam depth.

A typical load-deflection curve is shown in Fig. 5(a). According to ASTM C1609 (ASTM C1609/C1609M 2012), the peak flexural load P_p can be directly determined from the load-deflection curve. Deflection δ is a crucial parameter and is calculated as only 1/150 of the span length (i.e., $\delta = L/150$). The residual load P_{RS}, which represents the load after cracking, corresponds to this deflection. The area under the curve represents the toughness. T_R, which is the amount of resistance to material fracturing under stress. Toughness is measured in kN·mm or J units and is defined as the ratio of absorbable energy to the volume before complete material failure. The toughness of the specimen can be obtained by integrating the area under the load-deflection curve to $\delta = L/150$

$$T_R = \int_0^{L/150} P\delta(x)dx \tag{2}$$

By utilizing Eq. (2), it is possible to transform the P–δ curve into a curve that represents flexural strength (f) versus deflection (δ), as shown in Fig. 5(b). The conversion process involves using the following equations to obtain the peak flexural strength P_p and residual load P_{RS} from the peak flexural strength f_p and residual strength f_{RS}, respectively

$$f_{RS} = \frac{P_{RS}L}{bd^2} \tag{3}$$

$$f_P = \frac{P_P L}{bd^2} \tag{4}$$

The point at which the f–δ curve reaches its maximum load-bearing capacity under a limited load is known as the peak flexural strength, denoted as f_p. On the other hand, the flexural strength of the material after it has cracked at a deflection of $\delta = L/150$ on the f–δ curve is called the residual strength, denoted as f_{RS}. This residual strength represents the remaining load-bearing capacity of the

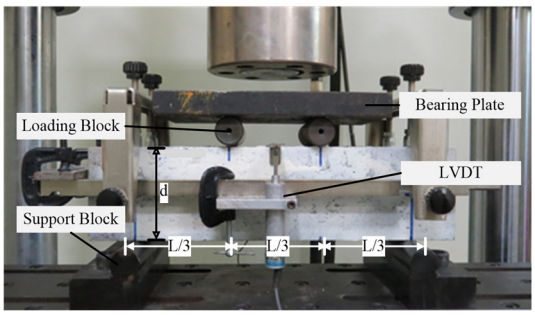

Fig. 4 Three-point flexural test

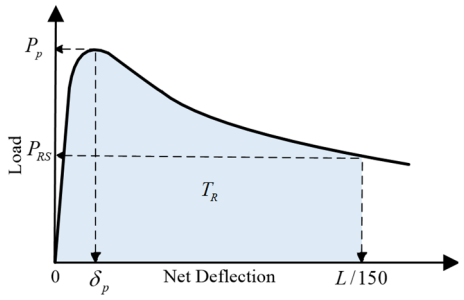

(a) load-deflection curve.

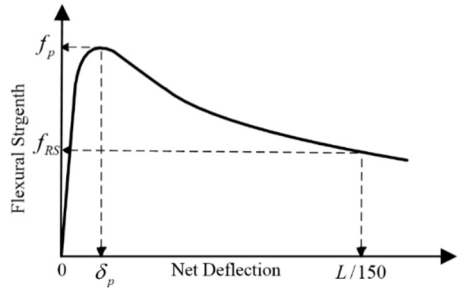

(b) flexural strength-deflection curve

Fig. 5 Typical (a) load-deflection curve and (b) flexural strength-deflection curve (ASTM C1609 2012)

material after cracking has occurred. The position of the residual strength on the curve is illustrated in Fig. 5(b).

3. Results and discussion

3.1 Fresh mixture properties and compressive strength

In UESFRC, superplasticizers reduce water consumption while maintaining high workability without compromising the cement hydration process. The superplasticizers act as solid barriers between the cement particles during the initial mixing process, stabilizing the dispersion process and separating the particles. Fine silica fume particles were added to the mix in this study to increase gradation uniformity and improve paste viscosity. The silica fume underwent a pozzolanic reaction, slowing cement volume contraction and resulting in stable late-stage strength (Johnston 1992).

Steel fibers were added to enhance the material's mechanical properties and reduce the fluidity of the concrete to a certain degree. However, a high fiber content increased the air content in the mix, which indirectly compromised the fluidity and workability of the cement. An extended mixing time was necessary to ensure the uniform distribution of steel fibers in the paste (Bayasi and Soroushian 1992), which increased the construction time of UESFRC. Hence, the quantity of steel fibers needed careful planning. Micro steel fibers were used to facilitate uniform fiber distribution in the concrete paste to prevent excessive slenderness ratios of fibers from causing fiber clots during the mixing process (Zuraida *et al*. 2011).

Following ASTM C143 (ASTM C143 2020) standards, a slump test was conducted after mixing, and each type of concrete was tested five times. Concrete slump is a crucial indicator of its strength and durability once solidified. As listed in Table 2, concrete bonding slurry was tested for slump; the results are shown in Table 2.

The results in Table 2 indicate that increasing the volume ratio of steel fibers decreased the flowability of the concrete bonding slurry. The slump reduction rate was 7.4% and 22.2% when adding steel fibers with a 0.5% and 1% volume ratio, respectively. Despite the slump reduction rate, the slump of UESFRC 1% was 210 mm, satisfying the compatibility requirement (Bayasi and Soroushian 1992). However, Bayasi's study found that adding a 1.5% volume ratio of steel fibers decreased the slump to 155 mm.

The compressive strength of concrete can be influenced by multiple factors, with the binding force between components being a significant one. The hydration levels of cement also impact the adhesive force between the mortar and coarse aggregate. During the initial hydration process, the interface between the two is weak, and the strength of the interface primarily depends on the level of mortar hardening. However, the adhesive force increases as hydration progresses, and the contact area between the two decreases, causing the coarse aggregate to produce a load (Golaszewski *et al*. 2019). The gradation of the mortar affects its fluidity and hydration rate, ultimately impacting the development of early strength and stability of late-stage strength (Engbert and Plank 2021). To optimize the mortar's density and improve its strength, this study used silica fume (Chore and Joshi 2021).

Table 2 Properties of the fresh UESFRC mortar

Slump (mm)	Max	Min	Average	Slump reduction rate
UESC	280	260	270	-
UESFRC (0.5%)	260	240	250	7.4%
UESFRC (1%)	220	200	210	22.2%

In steel fiber reinforced concrete, steel fibers are deliberately added to enhance various mechanical properties of concrete, including tensile strength, toughness, and durability. However, early-strength steel fiber concrete often exhibits a phenomenon known as "fiber effect delay (Shaalan *et al*. 2016)". During the initial stages of concrete hydration, the primary focus is on forming the cementitious matrix, and the concrete's mechanical properties are still evolving. While steel fibers are introduced into the mix during this phase, their immediate impact on the concrete's strength and other mechanical attributes may not be readily discernible. This is because the fibers are initially dispersed within the matrix without fully engaging in reinforcing the structure.

As the hydration process advances and the concrete gradually gains strength and stiffness, the role of steel fibers becomes more pronounced. They begin to reinforce the matrix actively, providing additional tensile strength and resistance to cracking. This delayed manifestation of the fiber effect is a common characteristic observed in early-strength SFRC. The full benefits of fiber reinforcement become increasingly evident as the concrete matures and the steel fibers contribute more substantially to its mechanical performance.

The compressive strengths of this study are presented in Table 3. All concrete materials exhibited compressive strengths through optimized mix designs at 4 hours of age. As time progressed, the compressive strength of the three concretes exceeded 35 MPa at 6 hours and surpassed 60 MPa after one day, which is significant. Notably, the steel fibers began to demonstrate their effect after three days. While the compressive strength of UESC was 72.7 MPa, the compressive strength of 0.5% and 1% UESFRC reached 81.7 MPa and 91.9 MPa, respectively. Subsequently, the strength development tended to slow down. At 28 days, when the strength stabilized, the compressive strength of UESC was 82.1 MPa, while the compressive strength of 0.5% and 1% UESFRC was 95.5 MPa and 107.8 MPa, respectively.

It is worth noting that some studies have indicated that adding more than 0.5% steel fiber can enhance compressive strength (Ghosh *et al*. 2021). This observation aligns with our findings, suggesting a consistent trend. The rationale behind this phenomenon lies in the behavior of specimens containing steel fibers under load. While Poisson's ratio effect tends to induce cracking, the wrapping and bridging effects of the steel fibers effectively mitigate crack propagation within the body, thereby contributing to

Table 3 Compressive strengths of various concrete mixes mixtures investigated

Age	Compressive Strength f_c (MPa)		
	UESC	UESFRC 0.5%	UESFRC 1%
4hr	23.5 ± 0.4	26.5 ± 1.2	26.4 ± 0.1
6hr	35.3 ± 2.1	40.4 ± 0.2	37.2 ± 1.1
1D	64.5 ± 0.6	66.3 ± 1.7	66.0 ± 1.0
3D	72.7 ± 1.8	81.7 ± 3.6	91.9 ± 1.2
7D	76.6 ± 2.1	89.2 ± 2.6	96.8 ± 3.1
28D	82.1 ± 10.3	95.5 ± 1.7	107.8 ± 2.1

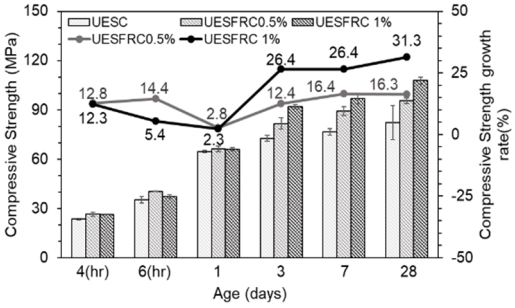

Fig. 6 Effects of steel fiber content on the compressive strength and compressive strength growth rate

increased compressive strength.

Table 3 shows the significant improvement in compressive strength resulting from the addition of straight steel fibers. In order to investigate the relationship between steel fiber content and strength growth, the UESFRC group was used as a baseline. Fig. 6 illustrates the impact of steel fiber content on both compressive strength and the rate of compressive strength growth. The formula used to calculate the growth rates of compressive strength G_R is as follows

$$G_R = \frac{X_x - X_0}{X_0} \times 100\% \quad (5)$$

Where X_x was the compressive strength at the time and X_0 was the compressive strength at 28 days.

In Fig. 6, there is no notable difference in the rate of compressive strength growth when steel fibers are utilized until after three days of age. This observation can be attributed to the fact that, although the ultra-early-strength concrete (UESC) matrix already possesses early strength surpassing that of normal concrete, the current capacity of the steel fibers for reinforcement is insufficient. Only after the initial 3-day period does the concrete substrate's stability gradually improve, allowing for a tighter bond with the steel fibers. Subsequently, the corresponding strength development becomes more pronounced.

Based on the results shown in Fig. 6, it can be observed that the concrete strength increases as the curing time increases. Different researchers have used various formulas to analyze the relationship between the compressive strength and age of ESC. For instance, Metwally (Abd Elaty 2014) utilized natural logarithmic equations to express this

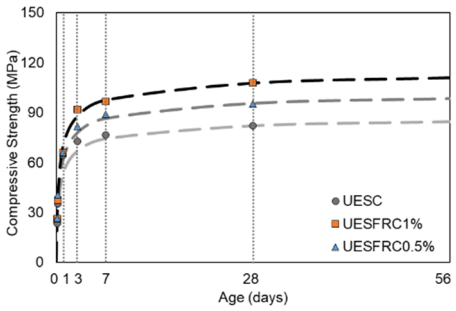

Fig. 7 Relationship between the compressive strength and age for concrete mixes

relationship. However, natural logarithms may not adequately describe the 1-day strength development of UESFRC. Moreover, 28 days is generally considered a benchmark for strength development stability, and at this point, conventional concrete reaches a strength of around 80% or higher (ACI 330R-08 2008). Nonetheless, for UESFRC, a 28-day curing period can lead to increased thermal and autogenous shrinkage issues due to early hydration and excessively rapid heat release. This, in turn, results in specimen cracking and affects the development of late-stage strength. To overcome these issues, steel fibers were used in this study to mitigate cracking resulting from concrete shrinkage, through the bridging effect of the steel fibers, which helped to resolve the problem of reduced late-stage strength. Haach *et al*. (2015) proposed the following equation to express the temporal function measured in days, depicting the relationship between the overall compressive strength of concrete at any age and its compressive strength on day 28, where *S* and *n* are constants

$$\dot{f}_c(t) = \dot{f}_{c,28d} \times e^{[S\left(1-(\frac{28}{t})^n\right)]} \quad (6)$$

A regression analysis was performed using Eq. (5) to examine the strength and age relationship of UESFRC, as illustrated in Fig. 7. The regression line equation used had *S* = 0.1 and *n* = 0.5. Results indicate that UESFRC exhibited a rapid strength increase during the first 24 hours, which continued for the following three days. After day 3, the rate of increase slowed, and the steel fibers maintained their strength. The compressive strengths of UESC, UESFRC 0.5%, and UESFRC 1% on day 28 were 12.9%, 16.9%, and 17.3% higher, respectively, compared to day 7, according to test results. The increase in late-stage compressive strength also led to an increase in the confinement effect produced by bonding between the steel fibers and concrete. This trend remained stable until day 56, suggesting that the strength development process of all three materials was nearly constant.

Fig. 8 depicts the failure modes of specimens under various test conditions, which were analyzed after conducting compression tests. Specimens without steel fibers remained intact after one day, but became increasingly brittle as the hydration process progressed. During the compression test, these specimens crumbled and collapsed under the compressive stress, with the fracture extending along the direction of the shear stress and leaving

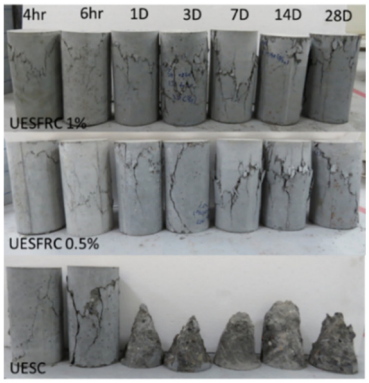

Fig. 8 Specimen failure modes of during compressive testing

a cone shaped fracture surface. However, specimens with steel fibers did not collapse after the compression test and retained their original shape. This is because steel fibers acted as bridges, maintaining the connection of the fragments at both ends of the crack after the matrix had cracked. This result confirms the effectiveness of steel fibers in reducing specimen failure under load, consistent with previous studies such as Naaman and Al-Khairi (Naaman and Al-Khairi 1996), which demonstrated that the inclusion of steel fibers can effectively enhance the load bearing capacity and toughness of concrete.

3.2 Flexural behavior of UESFRC

In this study, three different concrete types were tested for flexural strength, and the results are presented in Fig. 9, illustrating the failure modes. When observing the specimen from the side, it was evident that the UESFRC with added fibers exhibited a favorable bridging effect, as it remained intact even after breaking. On the other hand, the UESC without steel fibers fractured into two separate pieces. This characteristic is particularly significant for road bases that experience concentrated loads. It can be concluded that including steel fibers effectively enhances the concrete's resistance to direct breakage, providing a valuable preventive measure.

Upon comparing the three types of concrete sections, it was noted that the steel fibers in the cracks exhibited pulling rather than breaking, indicating that the added steel fibers possessed sufficient strength to bridge the damaged sections. Besides the primary cracks resulting from the flexural test, multiple micro-cracks were observed on the lower and lateral surfaces of the UESFRC beam specimen. These micro-cracks were formed due to the pulling action of the steel fibers and the substrate when the specimen was subjected to tension. The UESRC 1% exhibited a higher number and density of cracks than UESFRC 0.5%, suggesting that increased added steel fibers led to improved pulling effect and flexural strength properties.

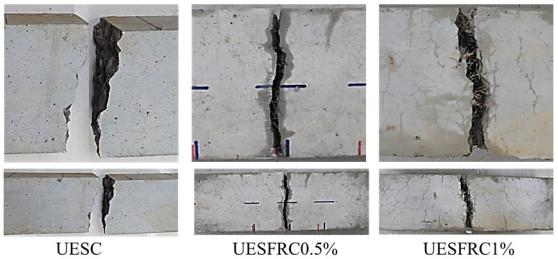

Fig. 9 Cracking modes of UESFRC specimen

The flexural strength versus deflection curves of three types of UESFRC at different ages was analyzed and presented in Fig. 10. Various construction projects, including airfield runways, have specific design requirements for flexural performance (UFC 2019). For instance, airfield runways necessitate concrete with flexural strength above 4.5 MPa (650 psi) compared to the general requirement of 3.8 MPa (550 psi). The study found that on day 1, UESC, UESFRC 0.5%, and UESFRC 1% attained flexural strengths of 7.5, 8.8, and 10.1 MPa, respectively, which satisfies the requirements of construction applications. The study further examined several aspects, such as the trends of curves during the strain hardening and softening phases, extreme flexural strength and corresponding deflection values, and the toughness, residual strength, and equivalent flexural strength values calculated using Eqs. (2) and (3).

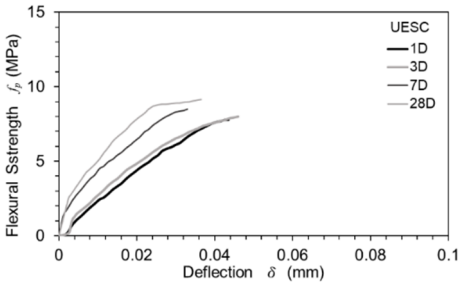

(a) UESC

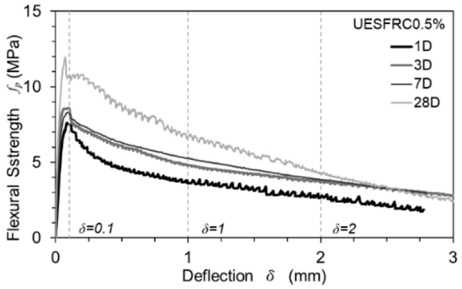

(b) UESFRC 0.5%

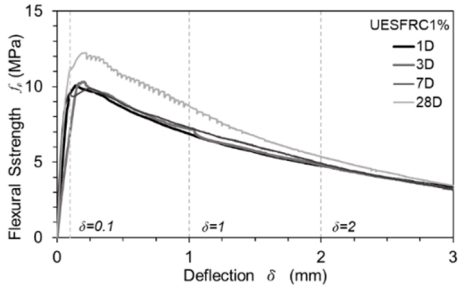

(c) UESFRC 1%

Fig. 10 Average flexural strength-–deflection curve: (a) UESC; (b) UESFRC 0.5%; and (c) UESFRC 1%

Table 4 Summary of basic fundamental flexural properties results

Age (Day)	Flexural strength f_p (MPa)			Deflection of average flexural strength δ_p (mm)			Toughness T_R (J)		
	UESC	UESFRC 0.5%	UESFRC 1%	UESC	UESFRC 0.5%	UESFRC 1%	UESC	UESFRC 0.5%	UESFRC 1%
1	7.5 ± 0.2	8.8 ± 1.5	10.1 ± 0.2	0.04	0.09	0.15	0.6	26.7	46.3
3	8.4 ± 0.5	8.6 ± 0.5	10.5 ± 0.1	0.05	0.10	0.20	0.8	34.6	46.4
7	8.1 ± 1.1	9.3 ± 0.5	10.3 ± 0.6	0.03	0.10	0.25	0.6	36.2	48.5
28	8.7 ± 1.1	12.0 ± 0.4	12.8 ± 1.9	0.04	0.07	0.22	0.8	47.5	56.7

The stiffness of the specimen increased with age before it cracked, as shown in Fig. 10. The material substrates of UESC specimens without steel fibers gradually hardened over the hydration process, but the overall deflection did not reach 0.1 mm when δ = 0.1 mm was used as a reference. However, the UESFRC specimens with steel fibers demonstrated increased flexural strength due to a bridging effect caused by the steel fibers, which deformed and pulled during the initial cracking phase. This was evidenced by the maximum strength of UESFRC 0.5% reached at δ = 0.1 mm and the corresponding deflection of the maximum strength of UESFRC 1% exceeding δ = 0.1 mm. The UESC specimens fractured directly due to the rapid development of cracks, while the UESFRC specimens exhibited localized microcracks before reaching the limit load, resulting in macroscopic cracks. The material also softened during continuous load application exceeding the limit load of the beam specimens, which substantially increased its toughness. This softening effect caused the curves to zigzag. The UESFRC 0.5% exhibited distinct phases of strain-hardening and softening in its curve, whereas the UESFRC 1% showed a smoother peak curve, suggesting that increasing the steel fiber content led to enhanced strain-hardening and higher flexural strength.

Table 4 lists the peak flexural strengths, deflection values corresponding to the peak strengths, and toughness values of the three materials. The peak flexural strength of UESC was 7–9 MPa. After day 3, the flexural strength of the specimen gradually stabilized. The peak flexural strength of UESFRC 0.5% ranged from 8 to 12 MPa. At all ages, the flexural strength of UESFRC 1% exceeded 10 MPa, and its strength increased after day 7. On day 28, the strength of the UESC specimens with steel fibers reached 12 MPa and higher. However, the deflection corresponding to the peak strength differed among materials with different steel fiber contents. The peak deflection represented the deformation of the material under load until the maximum strength was reached. A larger peak deflection represented higher material ductility. As indicated in Table 4, when the steel fibers' volume content increased, the specimen's peak deflection also increased. For example, the peak deflection of UESC was approximately 0.03–0.05 mm, demonstrating no significant differences. However, in specimens with steel fibers, the peak deflection was approximately 0.1 mm, with the peak deflection of UESFRC 1% even exceeding 0.15 mm. On day 3, the peak deflection reached 0.2 mm. These results indicated that after the concrete specimens with steel fibers exceeded the limit load, the observed softening

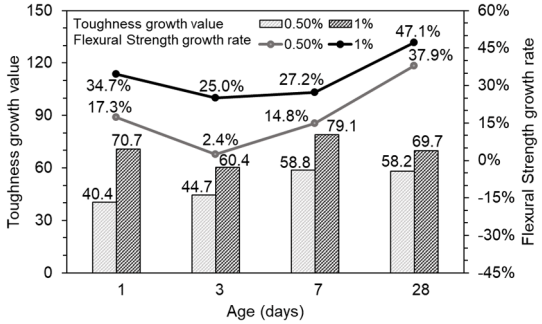

Fig. 11 Effects of steel fiber content on the toughness growth values and flexural strength growth rates

enhanced the material's ductility, improving its brittleness and durability.

To calculate the value of toughness T_R, Eq. (2) was employed, and the results were compared across various groups. Since the deflection of UESC without steel fibers did not reach δ = L/150, the area under the curve was determined by integration. The findings indicated that adding steel fibers provided clear advantages in terms of toughness T_R,. Specifically, the maximum T_R, value of materials without steel fibers was 0.8 J. In comparison, the toughness values of UESFRC 0.5% and UESFRC 1% were greater than 26 J and 46 J, respectively, highlighting the significant improvement in toughness achieved by incorporating steel fibers.

The growth rates and growth values of peak flexural strength and toughness of UESFRC specimens were calculated using Eq. (4) and presented in Fig. 11. On days 1, 3, 7, and 28, the flexural strength growth rates of UESFRC 0.5% were 17.3%, 2.4%, 14.8%, and 37.9%, respectively, with toughness growth values of 40.4, 44.7, 58.8, and 58.2, respectively. On days 1, 3, 7, and 28, the flexural strength growth rates of UESFRC 1% were 34.7%, 25.0%, 27.2%, and 47.1%, respectively, with toughness growth values of 70.7, 60.4, 79.1, and 69.7, respectively. The flexural strength growth rate decreases on the third day as the base material strength stabilizes, but the flexural strength growth rate increases after the base material hardens and the steel fibers come into play. On day 28, the addition of steel fibers enhanced the material's toughness, resulting in a peak in growth rates. The toughness growth values of UESFRC 0.5% and UESFRC 1% remained at 40–60 and 60–80, respectively, and late-stage toughness growth values remained constant as the age increased. The improvement

Table 5 Results of residual strength

Residual strength f_{RS} (MPa)					
Type	UESFRC 0.5%			UESFRC 1%	
δ (mm)	0.1	1	2	1	2
1D	7.5	3.62	2.69	6.87	4.78
3D	8.6	4.79	3.68	7.2	4.81
7D	8.3	6.68	3.86	8.73	4.92
28D	10.70	5.30	4.30	7.28	5.36
Strength reduction rate					
Type	UESFRC 0.5%			UESFRC 1%	
δ (mm)	0.1	1	2	1	2
1D	15%	59%	69%	32%	53%
3D	0.2%	44%	57%	31%	54%
7D	11%	28%	58%	15%	52%
28D	11%	52%	64%	43%	58%

in flexural properties caused by the addition of steel fibers was discernible, with a difference of approximately ten between the toughness growth values of UESFRC 0.5% and UESFRC 1%.

In compliance with ASTM C1609 standards, a residual flexural strength of $\delta = L/150$ was used to compare concrete specimens with and without steel fibers. The residual flexural strength represents the remaining bearing capacity of the specimen after the peak strength is reached and can be used to quantify the bridging effect of steel fibers. To investigate the residual strength, deflections of δ = 0.1, 1, and 2 mm were used, with the corresponding strengths labeled as $f_{RS,0.1}$, $f_{RS,1}$, and $f_{RS,2}$, respectively, as shown in Figs. 10(b) and (c). The rate of reduction of peak strength at the corresponding age is presented in Table 5, with the strength reduction rate calculated using the equation specified in the study. The results demonstrate that concrete specimens with steel fibers exhibit a certain degree of ductility due to the bridging effect, evident in the residual strengths observed for different deflections.The strength reduction rate R_S was calculated as follows

$$R_S = \frac{f_P - f_{RS,x}}{f_p} \times 100\% \quad (7)$$

According to the results in Fig. 10(c), UESFRC 1% demonstrated high flexural performance, and the flexural strength at δ = 0.1 mm did not yet pass the peak value, which would not meet the "residual" definition, and hence, the residual flexural strength and flexural strength reduction values were not discussed further. Table 5 presented the residual flexural strengths and strength reduction rates for UESFRC 0.5% and UESFRC 1%, where the $f_{RS,0.1}$ values at 1, 3, 7, and 28 days were 7.5, 8.6, 8.3, and 10.7 MPa, respectively, for UESFRC 0.5%, while the $f_{RS,1}$ values at the same ages were 3.6, 4.8, 6.7, and 5.3 MPa, respectively. The flexural strength reduction rate ranged from 28% to 60%, and the $f_{RS,2}$ values at the same ages were 2.7, 3.7, 3.9, and 4.3 MPa, respectively. The residual flexural strengths for UESFRC 0.5% exhibited small differences at

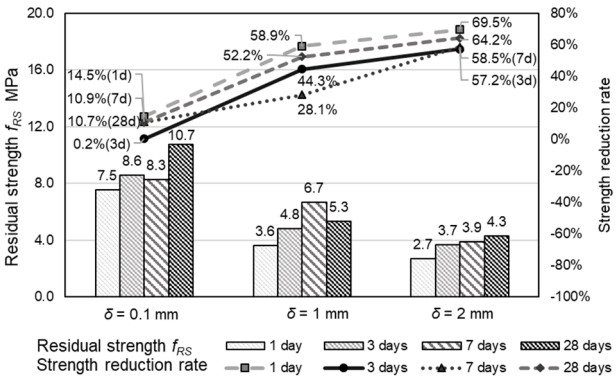

(a) UESFRC 0.5%

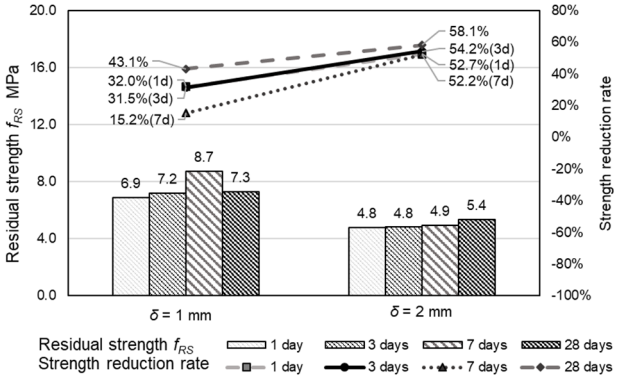

(b) UESFRC 1%

Fig. 12 Effects of steel fiber content on the residual strength and flexural strength reduction rates

all ages, with a flexural strength reduction rate of around 60%. For UESFRC 1%, the $f_{RS,1}$ values at 1, 3, 7, and 28 days were 6.9, 7.2, 8.7, and 7.3 MPa, respectively, with a flexural strength reduction rate of approximately 30%. The $f_{RS,2}$ values at the same ages were 4.8, 4.8, 4.9, and 5.4 MPa, respectively, with a flexural strength reduction rate of around 50%. Overall, the results indicated that increasing the volume of added steel fibers helped stabilize the strength reduction during the softening phase, and with a volume ratio of 1%, UESFRC 1% maintained a flexural strength of approximately 5 MPa with a deflection of 2 mm.

The effect of steel fibers on the flexural strength and residual strength of UESFRC was investigated in a study, with the residual flexural strength and strength reduction rate compared. The residual flexural strength was observed for fixed deformations of δ = 0.1, 1, and 2 mm, which highlights the material's ability to support flexural strength after entering the plastic stage post-cracking. The results in Fig. 12(a) and (b) demonstrated that increased steel fiber content could effectively suppress the strength reduction rate, with residual strength being maintained above 4.8 MPa at a deformation of δ = 2 mm, and the strength reduction rate less than 60%. Furthermore, the residual strength values were smaller for the earlier ages, while the residual strength reduction rate remained below 70% at δ = 2 mm, indicating more than 30% load-bearing capacity. This study shows that steel fibers can significantly enhance the residual strength and suppress the strength reduction rate of UESFRC.

4. Conclusions

This study introduced an innovative type of concrete called ultra-early-strength concrete (UESC), designed to achieve high strength quickly without the need for curing. To address the potential issue of microcracks resulting from rapid early strength development, the UESC was reinforced with steel fibers. By combining data from both experimental and analytical methods, we were able to draw the following conclusions:

- Through meticulous proportioning design and careful material selection, the ultra-early-strength concrete investigated in this study achieves a remarkable compressive strength of 20 MPa within a mere 4 hours, even without curing. Furthermore, it demonstrates impressive development, attaining a compressive strength of 69.6 MPa and a flexural strength of 7.5 MPa after just 24 hours. This significant advancement greatly benefits time-sensitive construction projects.
- The addition of steel fibers is intended to enhance the mechanical properties of UESC. While significant benefits from steel fibers were not observed in the early mechanical properties, the concrete substrate exhibited gradual strength stabilization and sufficient bond capacity by three days age, with the steel fibers exhibiting effective bridging effects. The addition of steel fibers greatly enhanced all aspects of the mechanical properties of UESC, and the strength gradually appeared as the volume ratio increased. At day 28, UESFRC 0.5% and 1% had 16.3% and 31.3% greater compressive strength than UESC, respectively; for flexural strength, the peak flexural strength increased by 37.1 and 47.9%, respectively; and the toughness also improved by 58.2 and 69.7 times, too. It showed that the addition of steel fibers significantly enhanced the ductility, toughness, and durability of the material.
- The specimen containing steel fibers maintained its structural integrity during the compression test due to the bridging effect of the fibers. Additionally, the flexural specimens showed resistance to splitting, preventing immediate material failure. This characteristic is crucial for applications such as tunnels and airport roads, as it helps prevent direct damage resulting from concentrated stresses.
- The inclusion of 0.5% steel fibers in UESC demonstrated the achievement of project specifications through enhanced mechanical properties. This finding highlights the feasibility of integrating steel fibers without compromising strength.

Acknowledgments

This research was funded in part by the MOH AND ASSOCIATES (MAA), Inc. The authors acknowledge the MAA for its financial support and the comments and suggestions made by its staff and project manager. Meanwhile, we would also like to thank CHING-TAI RESINS CHEMICAL CO. for the technical guidance and the chemicals provided. The opinions expressed in this paper are those of the writers and do not necessarily reflect the sponsor's views.

References

Abbas, S., Soliman, A.M. and Nehdi, M.L. (2015), "Exploring mechanical and durability properties of ultra-high performance concrete incorporating various steel fiber lengths and dosages", *Constr. Build. Mater.*, **75**, 429-441. https://doi.org/10.1016/j.conbuildmat.2014.11.017

Abd Elaty, M.A.A. (2014), "Compressive strength prediction of Portland cement concrete with age using a new model", *HBRC j.*, **10**(2), 145-155. https://doi.org/10.1016/j.hbrcj.2013.09.005

ACI 330R-08 (2008), Guide for the Design and Construction of Concrete Parking Lots; American Concrete Institute, Farmington Hills, MI, USA.

Altun, F., Haktanir, T. and Ari, K. (2007), "Effects of steel fiber addition on mechanical properties of concrete and RC beams", *Constr. Build. Mater.*, **21**(3), 654-661. https://doi.org/10.1016/j.conbuildmat.2005.12.006

Ananyachandran, P. and Vasugi, V. (2022), "Development of a sustainable high early strength concrete incorporated with pozzolans, calcium nitrate and triethanolamine: An experimental study", Sustainable Energy Technologies and Assessments, **54**, 102857. https://doi.org/10.1016/j.seta.2022.102857

Anderson, J. (2001), "4x4 Concrete", Caltrans & WSCACPA Concrete Pavement Conference.

ASTM C143/C143M-20 (2020), Standard Test Method for Slump of Hydraulic-Cement Concrete, ASTM International, West Conshohocken, PA, USA, pp. 1-2.

ASTM C1609/C1609M (2012), Standard Test Method for Flexural Performance of Fiber-Reinforced Concrete (Using Beam with Third-Point Loading), ASTM International, West Conshohocken, PA, USA, pp. 1-9.

ASTM C78/C78M (2021), Standard Test Method for Flexural Strength of Concrete (Using Simple Beam with Third-Point Loading), ASTM International, West Conshohocken, PA, USA, pp. 1-5.

Barros, J.A., Lourenco, L.A., Soltanzadeh, F. and Taheri, M. (2013), "Steel fibre reinforced concrete for elements failing in bending and in shear", *Adv. Concrete Constr., Int. J.*, **1**(1), 1-27. https://doi.org/10.12989/acc.2013.1.1.001

Bayasi, M.Z. and Soroushian, P. (1992), "Effect of steel fiber reinforcement on fresh mix properties of concrete", *Mater. J.*, **89**(4), 369-374. https://doi.org/10.14359/9751

Bhat, K.M.U.D. and Khan, M.Z. (2018), "Effect of Steel Fibre Reinforcement on Early Strength of Concrete", *Int. J. Trend Sci. Res. Dev.*, **2**, 198-225. https://doi.org/10.31142/ijtsrd15781

Bury, M.A. and Nmai, C. (2005), "Innovative admixture technology facilitates rapid repair of concrete pavements", In: *8th International Conference on Concrete Pavements American Association of State Highway and Transportation Officials* (*AASHTO*) *American Concrete Pavement Association Cement Association of Canada Colorado Department of Transportation Concrete Reinforcing Steel Institute Federal Highway Administration Portland Cement Association Purdue University Transportation Research Board*, pp. 441-452.

Chore, H.S. and Joshi, M.P. (2021), "Strength properties of concrete with fly ash and silica fume as cement replacing materials for pavement construction", *Adv. Concrete Constr., Int. J.*, **12**(5), 419-427. https://doi.org/10.12989/acc.2021.12.5.419

Dai, L., Wang, L., Bian, H., Zhang, J., Zhang, X. and Ma, Y. (2019), "Flexural capacity prediction of corroded prestressed concrete beams incorporating bond degradation", *J. Aerosp. Eng.*, **32**(4), 04019027. https://doi.org/10.1007/s10973-017-6837-8

Engbert, A. and Plank, J. (2021), "Impact of sand and filler materials on the hydration behavior of calcium aluminate cement", *J. Am. Ceramic Soc.*, **104**(2), 1067-1075. https://doi.org/10.1111/jace.17505

Eskandarsefat, S. (2018), "Investigation on the effects of mix water temperature on High-Early strength cement concrete properties–An experimental work and a case study", *J. Build. Eng.*, **20**, 208-212. https://doi.org/10.1016/j.jobe.2018.07.023

FAA AC 150-5370-10H (2018), Standard Specifications for Construction of Airports; U.S. Department of Transportation.

Flatt, R. and Schober, I. (2012), "Superplasticizers and the rheology of concrete", In: *Understanding the rheology of concrete*, pp. 144-208. https://doi.org/10.1533/9780857095282.2.144

Ghosh, D., Abd-Elssamd, A., Ma, Z.J. and Hun, D. (2021), "Development of high-early-strength fiber-reinforced self-compacting concrete", *Constr. Build. Mater.*, **266**, 121051. https://doi.org/10.1016/j.conbuildmat.2020.121051

Golaszewski, J., Cygan, G. and Golaszewska, M. (2019), "Development and optimization of high early strength concrete mix design", In: *IOP Conference Series*: *Materials Science and Engineering*, **471**(11), 112026. https://doi.org/10.1088/1757-899X/471/11/112026

Haach, V.G., Juliani, L.M. and Da Roz, M.R. (2015), "Ultrasonic evaluation of mechanical properties of concretes produced with high early strength cement", *Constr. Build. Mater.*, **96**, 1-10. https://doi.org/10.1016/j.conbuildmat.2015.07.139

Haido, J.H., Abdul-Razzak, A.A., Al-Tayeb, M.M., Bakar, B.H., Yousif, S.T. and Tayeh, B.A. (2021), "Dynamic response of reinforced concrete members incorporating steel fibers with different aspect ratios", *Adv. Concrete Constr., Int. J.*, **11**(2), 89-98. https://doi.org/10.12989/acc.2021.11.2.089

Johnston, C.D. (1992), "Durability of high early strength silica fume concretes subjected to accelerated and normal curing", *Special Publication*, **132**, 1167-1188. https://doi.org/10.14359/1222

Kaïkea, A., Achoura, D., Duplan, F. and Rizzuti, L. (2014), "Effect of mineral admixtures and steel fiber volume contents on the behavior of high performance fiber reinforced concrete", *Mater. Des.*, **63**, 493-499. https://doi.org/10.1016/j.matdes.2014.06.066

Kanchanason, V. and Plank, J. (2018), "Effectiveness of a calcium silicate hydrate–Polycarboxylate ether (CSH–PCE) nanocomposite on early strength development of fly ash cement", *Constr. Build. Mater.*, **169**, 20-27. https://doi.org/10.1016/j.conbuildmat.2018.01.053

Kim, Y., Hanif, A., Usman, M., Munir, M.J., Kazmi, S.M.S. and Kim, S. (2018), "Slag waste incorporation in high early strength concrete as cement replacement: Environmental impact and influence on hydration and durability attributes", *J. Cleaner Production*, **172**, 3056-3065. https://doi.org/10.1016/j.jclepro.2017.11.105

Kontoni, D.P.N., Jahangiri, B., Dalvand, A. and Shokri-Rad, M. (2023), "Effect of length and content of steel fibers on the flexural and impact performance of self-compacting cementitious composite panels", *Adv. Concrete Constr., Int. J.*, **15**(1), 23-39. https://doi.org/10.12989/acc.2023.15.1.023

Kroviakov, S., Kryzhanovskyi, V. and Zavoloka, M. (2021), "Steel fibrous concrete with high-early strength for rigid pavements repair", *IOP Conference Series*: *Materials Science and Engineering*, **1162**(1), 012008. https://doi.org/10.1088/1757-899X/1162/1/012008

Kumar, R., Samanta, A.K. and Roy, D.S. (2014), "Characterization and development of eco-friendly concrete using industrial waste–A Review", *J. Urban Environ. Eng.*, **8**(1), 98-108. https://www.jstor.org/stable/26203414

Kumar, D.P., Amit, S. and Chand, M.S.R. (2021), "Influence of various nano-size materials on fresh and hardened state of fast setting high early strength concrete [FSHESC]: A state-of-the-art review", *Constr. Build. Mater.*, **277**(29), 122299. https://doi.org/10.1016/j.conbuildmat.2021.122299

Lee, T.Y. (2020), "4x4™ Concrete Very High-Early Strength Concrete Admixture", CHING-TAI RESINS CHEMICAL CO., LTD.

Li, M. and Li, V. (2011), "High-Early-Strength Engineered Cementitious Composites for Fast, Durable Concrete Repair-Material Properties", *ACI Mater. J.*, **108**(1), 3-12. https://doi.org/10.14359/51664210

Liu, Y., Jia, M., Song, C., Lu, S., Wang, H., Zhang, G. and Yang, Y. (2020), "Enhancing ultra-early strength of sulphoaluminate cement-based materials by incorporating graphene oxide", *Nanotechnol. Rev.*, **9**(1), 17-27. https://doi.org/10.1515/ntrev-2020-0002

Master Builders Solutions (2020), Master Builders Solutions Concrete Admixtures. https://www.master-builders-solutions.com/r-d/focus-on-innovation

Naaman, A.E. and Al-Khairi, F.M. (1996), "Bending Properties of High-Early-Strength Fiber Reinforced Concrete", *Special Publication*, **159**, 351-374. https://doi.org/10.14359/1430

Nayaka, R., Diwakar, G.S. and Gudur, V. (2018), "Effect of steam curing on the properties of high early strength silica fume concrete", In: *IOP Conference Series*: *Materials Science and Engineering*, **431**(4), 042011. https://doi.org/10.1088/1757-899X/431/4/042011

Nkinamubanzi, P-C., Mantellato, S. and Flatt, R.J. (2016), "Superplasticizers in practice", In: *Science and Technology of Concrete Admixtures*, pp. 353-377. https://doi.org/10.1016/B978-0-08-100693-1.00016-3

Pansuk, W., Nguyen, T.N., Sato, Y., Den Uijl, J.A. and Walraven, J.C. (2017), "Shear capacity of high performance fiber reinforced concrete I-beams", *Constr. Build. Mater.*, **157**, 182-193. https://doi.org/10.1016/j.conbuildmat.2017.09.057

Shaalan, H., Ismail, M.A.M. and Azit, R. (2016), "Time-dependent behavior of steel fiber reinforced shotcrete lining under rock overstressing using shotcrete model", *Electron. J. Geotech. Eng. EJGE*, **21**(26), 10365-10378. https://web.archive.org/web/20180426060626id_/http://www.ejge.com/2016/Ppr2016.0807ma.pdf

Sunarno, Y., Rangan, P.R. and Tumpu, M. (2023), "Effect of Accelerators on High Early Strength Concrete (HESC) Using High Volume Fly Ash", In: *IOP Conference Series*: *Earth and Environmental Science*, **1272**(1), 012025. https://doi.org/10.1088/1755-1315/1272/1/012025

Tang, C.W. (2021), "Mix design and early-age mechanical properties of ultra-high performance concrete", *Adv. Concrete Constr., Int. J.*, **11**(4), 335-345. https://doi.org/10.12989/acc.2021.11.4.335

UFC 3-260-01 (2019), Airfield and Heliport Planning and Design; Department of Defense, USA.

Wang, S. and Li, V.C. (2006), "High-early-strength engineered cementitious composites", *ACI Mater. J.*, **103**(2), 97. https://doi.org/10.14359/15260

Wang, S., Liu, B., Zhao, P., Lu, L. and Cheng, X. (2018), "Effect of early-strength-enhancing agents on setting time and early mechanical strength of belite–barium calcium sulfoaluminate cement", *J. Thermal Anal. Calorim.*, **131**, 2337-2343. https://doi.org/10.1007/s10973-017-6837-8

Wu, Z., Shi, C., Khayat, K.H. and Wan, S. (2016), "Effects of different nanomaterials on hardening and performance of ultra-

high strength concrete (UHSC)", *Cement Concrete Compos*., **70**, 24-34. https://doi.org/10.1016/j.cemconcomp.2016.03.003

Wu, Y., Li, Q., Li, G., Tang, S., Niu, M. and Wu, Y. (2021), "Effect of naphthalene-based superplasticizer and polycarboxylic acid superplasticizer on the properties of sulfoaluminate cement", *Materials*, **14**(3), 662. https://doi.org/10.3390/ma14030662

Xia, L., Zhou, M., Ni, T. and Liu, Z. (2020), "Synthesis and characterization of a novel early-strength polycarboxylate superplasticizer and its performances in cementitious system", *J. Appl. Polym. Sci*., **137**(30), 48906. https://doi.org/10.1002/app.48906

Yasin, A.K., Bayuaji, R., and Susanto, T.E. (2017), "A review in high early strength concrete and local materials potential", *IOP Conference Series*: *Materials Science and Engineering*, **267**(1), 012004. https://doi.org/10.1088/1757-899X/267/1/012004

Zuraida, A., Sopyan, I. and Zahurin, H. (2011), "Effect of fiber length variations on properties of coir fiber reinforced cement-albumen composite (CFRCC)", *IIUM Engineering. J*., **12**(1), 65-77. https://doi.org/10.31436/iiumej.v12i1.116